Articles

Estimation of Volume of Distribution in Humans from High Throughput HPLC-Based Measurements of Human Serum Albumin Binding and Immobilized Artificial Membrane Partitioning

Ferenc Hollósy,[†,‡] Klára Valkó,*[,†] Anne Hersey,[†] Shenaz Nunhuck,[†] György Kéri,[‡] and Chris Bevan[†]

Computational, Analytical and Structural Sciences, GlaxoSmithKline, Gunnels Wood Road, Stevenage, Hertfordshire, SG1 2NY United Kingdom, and Cooperative Research Centre, Semmelweis University Budapest, Üllöi út 26, 1088 Budapest, Hungary

Received September 26, 2005

The volume of distribution (VD) in humans of 179 known drug molecules (acids, bases, and neutrals) has been modeled using two biomimetic-binding measurements. The phospholipid binding (log *K* (IAM)) and the plasma protein binding (log *K* (HSA)) have been calculated from gradient HPLC retention times on immobilized artificial membrane (IAM) and on human serum albumin (HSA) columns, respectively. The log VD values showed good correlation with the compounds' relative binding to IAM and HSA as follows: log VD = 0.44 log *K* (IAM) − 0.22 log *K* (HSA) − 0.66; $n = 179$, $r^2 = 0.76$, $s = 0.33$, and $F = 272$. It was also observed that positively charged molecules bind relatively more to IAM, while negatively charged ones bind more to HSA, in line with the empirical observation that bases tend to have a larger volume of distribution than acids. These results suggest that with the help of these two simple high throughput HPLC-based biomimetic binding measurements an important in vivo drug disposition property can be estimated for use in early drug discovery.

Introduction

As discovery chemistry produces increased numbers of potential drug candidates, the simultaneous optimization of multiple properties is becoming increasingly important in the drug selection and promotion process. The massive increase in the cost of drug development, however, forces an early drastic selection of those molecules that display the greatest likelihood of success.

The ideal situation for the pharmaceutical industry would be that the human metabolism and pharmacokinetics (PKs) of a drug candidate compound can be predicted based on solely its molecular structure and physicochemical properties.[1,2] Physicochemical properties used today in early drug discovery programs include solubility, lipophilicity, molecular size, hydrogen-bonding capacity, and charge, all of which are considered as important features because they relate to various aspects of absorption, distribution, metabolic stability, and excretion (ADME).[3−6] However, there are no general rules for their application, which is the dominant property in any situation. Those compounds that fail to demonstrate satisfactory ADME properties and desirable PK profiles can be quickly removed from consideration as drug candidates.

Furthermore, screening large numbers of compounds for ADME/PK properties, especially using animals,[7,8] is a time-consuming, labor-intensive, and ethically sensitive process, which limits its utility in drug discovery. Therefore, those relatively simple in vitro physicochemical measurements in the initial evaluation phases that can provide a rapid selection of compounds with adequate bioavailability and acceptable ADME/PK properties are important.

In this paper, we investigate how the application of simple physicochemical measurements can be applied to model the volume of distribution (VD).

The VD is a theoretical concept that relates the administered dose to the plasma concentration. Most commonly it is calculated from the area under the curve (AUC) when plotting the plasma concentration as a function of time and the area under the moment curve to infinity (AUMC), and it is referred to as the volume of distribution at steady state (VD_{ss}).

$$VD_{ss} = \text{dose} \times \text{AUMC}/(\text{AUC})^2 \quad (1)$$

When a plasma concentration−time profile after intravenous injection of the drug exhibits a biexponential decline and the body can be viewed as a two-compartment model, an apparent VD can be derived from the AUC (VD_{area}) and can be obtained by eq 2.

$$VD_{area} = \text{dose}/k \times \text{AUC} \quad (2)$$

where k is the rate of clearance.

It was found that when using PKs to make drug dosing decisions, the difference between VD_{area} and VD_{ss} is not usually clinically significant.[9]

As an approximation, VD can be considered as a measure of the extent of distribution of a drug from plasma into tissues. The knowledge of VD together with the clearance determines the half-life of a drug, which is indicative of the duration of drug exposure.[10] Low values of VD mean that with smaller doses higher plasma concentration can be achieved. However, low VD with high clearance indicates shorter half-life, which means one has to apply the drug more frequently to achieve

* Corresponding author. Phone: +44 1438 763309. Fax: +441438763352. E-mail: klara.l.valko@gsk.com.
† GlaxoSmithKline.
‡ Semmelweis University Budapest.

10.1021/jm050957i CCC: $33.50
Published on Web 10/27/2006

the required level of plasma concentration. Drugs belonging to various therapeutic areas require different plasma concentration and tissue partition to achieve the desired efficacy and duration of action, therefore, the VD has to be optimized for each targeted pharmacological activity.

The VD of a compound depends on the volumes of the plasma and tissues and the ratio of the bound and unbound drug in plasma and tissue, that is, the plasma and tissue partition coefficients of the compounds. When we know the VD and the plasma protein binding (PPB), the tissue binding can be estimated by the Øie−Tozer[11] equation. Therefore, models developed to estimate VD can be used to estimate tissue distribution as well by taking into account the PPB.

The optimization of these pharmacodynamic and PK parameters was usually carried out at later stages of the drug development process. However, there is a trend to investigate these properties during the lead optimization and candidate selection processes to avoid the attrition of compounds during the more expensive development stage. Measurements of VD imply in vivo experiments that cannot be carried out on large number of compounds. Simple biomimetic partition measurements that are able to estimate this in vivo parameter without animal experiments therefore are of great value.

Various methods have been proposed to characterize VD including allometric species scaling,[12−14] direct scaling from human tissue in vitro, and scaling from animal and human tissue in vitro combined with species scaling.[15−17]The allometric scaling predicts the p*K* parameters for human from in vivo animal data on the basis of body weight.[17,18] These techniques employ the application of scaling factors such as protein binding, brain weight,[19] or maximum life span potential,[13] as well as various normalization methods.[12,14] However, although allometric scaling is simple and easy to handle, it does not always give accurate predictions for all drugs, and there are problems with its application to a wide variety of compounds.[20] The selection of the animal species may also influence the predictions.

A new approach defined as fractal VD, which scales the numerical values of VD proportionally to the body mass, was introduced and found to give better results than interspecies allometric scaling.[21,22]

In addition to these approaches, further methods to predict VD are the physiologically based PK (PBPK) modeling[23−26] and computational (in silico) approaches.[27−31] PBPK uses models of an organism that consists of several organs described by mass balance equations with their organ volume, organ blood flow, tissue to plasma partition coefficients, and permeation and transport terms as inputs. In PBPK models, VD of a drug in the body at steady state (VD_{ss}) can be calculated as a sum of volume of tissues (V_t) into which a drug distributes multiplied by the corresponding tissue−plasma partition coefficient ($P_{t/p}$) in addition to the plasma volume (V_p), resulting in the following equation:[7]

$$VD_{ss} = V_p + \sum P_{t/p} \times V_t \qquad (3)$$

Various models have been proposed to predict $P_{t/p}$ such as empirical, semi-empirical, tissue composition based in vivo or in vitro based types, which have been discussed in detail in several excellent review papers.[24,32−38]

The mechanistic approach helps the structure design process by systematically changing compound lipophilicity and PPB.[1,39,40] The tissues and plasma are considered as mixtures of lipids, water, and proteins, with an overall pH of 7.4. A drug partitioning into membrane lipid and water fractions as well as a reversible binding to the main plasma proteins and tissue interstitial space, are the processes currently considered for calculating the $P_{t/p}$ at the organ level.[17,41] Although tissue distribution is a key parameter driving the disposition of a drug, the lack of general models to estimate $P_{t/p}$ without extensive experimental work prevented the application of PBPK modeling in early drug discovery and development.

Changes in plasma affinity and resulting changes in unbound fraction can cause a large change in VD, which is reflected in only a relatively small change in the concentration of drug in tissue.[42] The relationship between PPB, tissue affinity, and VD_{ss} is described in eq 4.

$$VD_{ss} = V_p + \sum V_t \times f_u/f_{ut} \qquad (4)$$

where f_u is the fraction unbound in plasma and f_{ut} is the fraction of the drug that is unbound in tissue.

Because the half-life of a drug is determined by VD and clearance ($t_{1/2} = 0.693 \times$ VD/clearance), manipulation of VD (and clearance) is an important tool for changing the duration of the action.

More recently, a promising new approach has been published by Lombardo and co-workers,[43,44] using the Øie−Tozer equation,[11,45] which describes a relationship between VD_{ss} and f_{ut} in tissues. By measuring in vitro *E* log *D*[46] at pH 7.4, $f_{i(7.4)}$, the fraction ionized at pH 7.4 and PPB, a good estimate of the in vivo VD was obtained, yielding approximately a 2-fold improvement in mean accuracy. They found very good correlation ($R^2 > 0.86$) between the observed and the predicted fraction unbound in tissue (log f_{ut}) values for a set of 120 structurally diverse drugs. However, the predicted versus the measured VD_{ss} showed weaker correlation ($R^2 = 0.60$), and their model was applicable only for basic and neutral compounds.

Another model for the VD has recently been presented by Bayer AG based on measurements of membrane affinity and PPB using the Transil technology.[47] However, the details of the model have not been published for commercial reasons as it is built into the PK-SIM software.[48,49] The model uses the immobilized artificial membrane (IAM) partitioning and human serum albumin (HSA) binding data obtained by Transil technology to estimate VD and partition of compounds in various tissues such as liver, brain, lungs, heart, and so on.

Our mechanistic approach to model in vivo VD is based on the Brodie theory,[50] which highlighted the importance of the proportion of the compound's partition coefficient between the free solution and the plasma as well as the free solution and the tissues. Stated in logarithmic terms, it employs the difference between the logarithmic tissue and the plasma partition coefficients and is illustrated by Figure 1.

Although tissues contain a large amount of proteins (including albumin), they also contain large amounts of membranes and other lipid-containing components. The plasma contains a large amount of serum albumin (~670 μM) and much smaller amounts of α1-acid glycoprotein (10−20 μM in normal conditions), other globulins, and lipoproteins.[51]

Considering the earlier findings that PPB and membrane/lipid partition are the major driving forces for a solute's distribution into the body,[52] it offers an excellent opportunity to predict VD from HPLC-based biomimetic binding data using IAM columns and chemically bonded HSA stationary phases. For this reason, we have collected a diverse set of 179 known drug (acidic, basic, neutral, and zwitterionic) molecules for which reliable human VD and protein binding data were available in the literature

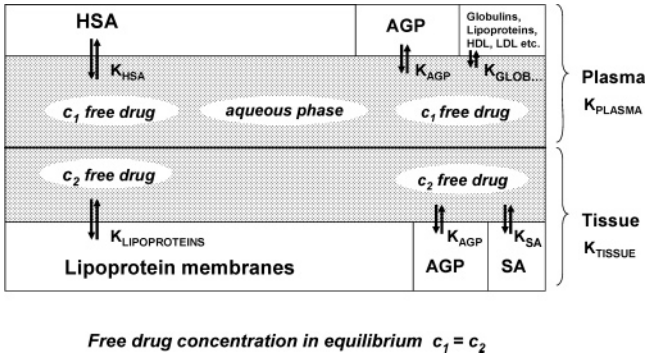

Figure 1. The VD can be described by the ratio of compounds' partition coefficients in plasma (K_{PLASMA}) and tissues ($K_{TISSUES}$).

from clinical studies. The HSA binding and IAM partition were measured, and these data have been related to the human VD data taken from the literature.

Results and Discussion

We have assembled VD data from clinical studies and PPB data for a set of 179 known drug molecules comprising acidic, basic, neutral, and zwitterionic drugs to build a predictive model that would not depend on any data requiring animal experiments. (See Table 1a,b in Supporting Information for the VD and PPB data with the reference sources[53−70]). When the VD data were obtained after oral administration of the drug, the bioavailability was taken into account. The volumes of distribution data obtained by various methods (intravenous, oral, or intramuscular administration) are not considered clinically significant. For example, literature values ranged from 10.4 to 13.6 liters and 50 to 60 liters for aspirin and Tamoxifen, respectively. In a log VD term, the differences are 0.11 and 0.08. This represents only approximately one-third of the root-mean-square error of our models. Some discrepancies reached over two mean-fold error, which is approaching the error of our models. As the models were not significantly different from the two subsets of compounds, we have merged them together (see Supporting Information for more details). We consider this set as a reasonably large, diverse, and representative set of known drug molecules suitable to develop a general model.

The basic principle of using chromatographic retention to measure the extent a compound partitions between the mobile and the stationary phase is well established. The binding constants can be derived from retention time measurements that can be measured very precisely. The measurements can easily be automated, and the presence of resolved impurities does not affect the results. We recognize that an overall binding parameter is obtained by this method, which includes specific and nonspecific binding.

It was described previously that the IAM lipophilicity scale is very similar to the octanol/water lipophilicity scale for neutral compounds based on the similarity of their solvation equations.[71] The effect of charge on the interaction with IAM was also studied at various pHs. It was found that positively charged compounds bound stronger to IAM than would be expected from octanol/water distribution.

We have also reported the introduction of a fast gradient HPLC method to determine HSA binding of discovery compounds using chemically bonded protein stationary phases.[72] We have shown that the HPLC-based HSA binding data correlate with the PPB data. Kratochwill and co-workers[39] have compared our published HPLC-based data with HSA affinity constants and found good correlation ($r^2 = 0.89$) between the binding constants obtained by HPLC and traditional ultrafiltration methods. Furthermore, the obtained HSA binding of known drug molecules was compared with the IAM binding data.[72,73] We found that although both HSA binding and IAM partition are mainly governed by lipophilicity, the presence of positive and negative charges makes the two types of binding very different. Such an effect can also be seen when we plot the two binding constants against each other (see Figure 2 and, for measured data, Table 1a,b).

It was observed that negatively charged compounds bind more strongly to HSA than would be expected from the lipophilicity of the ionized species at pH 7.4. While un-ionized molecules partitioning into IAM showed good correlation with octanol/water partition (log P), positively charged compounds showed a higher partition than expected from their octanol/water distribution. In contrast, the HSA binding of acidic compounds was much stronger than expected from their octanol/water distribution coefficients. These results suggest that the octanol/water distribution coefficients at physiological pH (log D_{ow}) are an inadequate parameter to predict the partition of ionized compounds (both acids and bases) in biological membranes and serum albumin.[73] Our present findings are in agreement with those of Herbette et al. and Kaliszan et al.[74,75]

We have investigated whether the above-described biomimetic partition data are suitable to model the tissue binding (IAM) and the plasma binding (HSA).

Based on the Brodie theory[50] and eq 4, we assume that the difference between the logarithmic value of the tissue and the plasma partition coefficients is equal to the logarithmic value of the VD (log VD $= a \times \log K_{TISSUE} - b \times \log K_{PLASMA}$), and eq 5 can then be set up.

$$\text{Log VD} = a \times \log K\,(\text{IAM}) - b \times \log K\,(\text{HSA}) + c \quad (5)$$

Of course, we know that this model is an oversimplification of the in vivo situation as tissues also contain proteins, such as albumin, and plasma contains other proteins, like AGP. However, we assume that HSA and IAM binding are the dominant factors that govern drug distribution processes and cause major differences between the plasma and tissue partition coefficients (Figure 1.)

The perfect model would contain binding data for all constituents in the plasma and the tissues, which would require more commercially available protein and lipid stationary phases. We have also considered including AGP binding into the model, but a strong correlation was found between IAM and AGP binding data for the set of compounds investigated (data not shown). For this reason only, IAM partition data was considered in the model (see Supporting Information for further details).

Substituting the data for the 179 compounds, eq 6 was obtained by multiple linear regression (MLR) analysis.

$$\text{Log VD} = 0.44(\pm 0.02) \log K\,(\text{IAM}) - 0.22(\pm 0.02) \log K\,(\text{HSA}) - 0.66 \quad (6)$$

where $N = 179$, $r^2 = 0.76$, $s = 0.33$, and $F = 272$.

The plot of the literature and calculated log VD values based on eq 6 can be seen in Figure 3. The model covers a wide range of the VD. Compounds like Dothiepin, Tamoxifen, and Maprotiline had the highest VD, 70, 55 and 53 L/kg, respectively, used in the model. We have tried to measure Amiodarone as well, for which the reported volume data were in the range of 66 to 71 L/kg. The HSA binding of Amiodarone was around 98% (log K (HSA) = 4.39). The IAM binding was also very

Table 1. Measured Parameters of the Investigated Drug Molecules in the Training Set and in the Test Set[a]

No	drug	CHI pH 2.0	CHI pH 7.4	CHI pH 10.5	delta CHI neg chrg	delta CHI pos chrg	CHI IAM	log *K* (IAM)	HSA %	log *K* (HSA)
					(a) Training Set					
1	Acecainide	13.3	21.3	42.5	0.0	21.2	23.3	2.00	29.8	0.69
2	Acetaminophen	17.4	16.8	−30.6	0.0	0.0	4.0	1.24	14.0	0.45
3	Acetanilide	42.0	41.2	41.8	0.0	0.6	10.7	1.43	25.3	0.62
4	Acetazolamide	39.9	33.3	21.0	6.5	0.0	−0.5	1.14	71.5	1.47
5	Alclofenac	72.9	39.4	36.2	33.5	0.0	17.8	1.71	98.7	5.11
6	Alosetron HCl	29.0	45.3	49.0	0.0	3.7	32.7	2.69	75.5	1.60
7	Amantadine	65.9	60.1	61.2	0.0	1.0	31.4	2.58	65.5	1.31
8	Amiloride	12.5	18.6	15.7	0.0	0.0	30.7	2.52	20.0	0.54
9	Amoxapine	36.4	61.5	89.6	0.0	28.1	52.7	5.69	86.2	2.15
10	Amoxicillin	40.9	18.1	8.4	22.8	0.0	6.3	1.30	16.4	0.49
11	Ampicillin	33.6	31.5	27.0	0.0	0.0	6.3	1.30	21.2	0.56
12	Apomorphine HCl	22.9	49.5	78.6	0.0	29.1	39.7	3.45	90.8	2.58
13	Aspirin	56.7	19.7	14.9	37.0	0.0	−1.7	1.12	37.3	0.79
14	Bamethan	14.6	24.0	42.4	0.0	18.4	18.6	1.75	16.5	0.49
15	Betamethasone	59.7	57.6	59.7	2.1	2.1	31.7	2.61	55.6	1.09
16	Bromazepam	44.1	54.2	56.3	0.0	2.1	28.5	2.34	68.5	1.38
17	Bromocriptin	49.1	91.6	93.0	0.0	1.4	47.9	4.70	94.1	3.13
18	Budesonide	77.2	75.0	76.6	2.2	1.6	38.7	3.32	78.7	1.73
19	Bumetanide	76.0	49.1	45.2	26.8	0.0	26.1	2.18	94.3	3.15
20	Carbamazepine	39.0	68.2	83.6	0.0	15.4	39.2	3.39	83.8	1.99
21	Cefazoline	39.3	22.0	22.8	17.3	0.0	2.5	1.21	62.7	1.24
22	Cefixime	30.0	13.8	10.3	16.2	0.0	−3.8	1.08	69.1	1.40
23	Cephalexin	21.6	23.8	23.8	0.0	0.0	−2.3	1.11	14.0	0.45
24	Chlorpheniramine	28.1	55.3	98.6	0.0	43.3	47.2	4.58	61.0	1.20
25	Chlorpropamide	68.2	34.9	33.0	33.3	0.0	5.8	1.29	91.6	2.68
26	Chlorprothixene	111.2	112.5	113.0	0.0	0.6	53.5	5.89	98.0	4.57
27	Cinoxacin	46.7	15.6	12.5	31.1	0.0	1.6	1.19	60.1	1.18
28	Clonazepam	66.5	66.2	65.1	0.3	0.0	34.8	2.90	77.1	1.66
29	Clonidine	15.1	34.3	53.2	0.0	18.9	28.8	2.37	28.0	0.66
30	Cloxacillin	73.4	45.7	43.5	27.7	0.0	23.1	1.99	92.7	2.86
31	Colchicine	46.8	44.8	47.5	2.0	2.6	23.7	2.02	37.1	0.79
32	Cytarabine	−45.2	−21.7	−27.1	0.0	0.0	−15	0.93	29.8	0.69
33	Diazepam	70.9	80.6	82.3	0.0	1.7	37.4	3.18	93.2	2.94
34	Diazoxide	49.2	47.7	27.8	1.5	0.0	24.7	2.08	75.2	1.59
35	Diclofenac	89.3	52.1	49.1	37.2	0.0	33.5	2.77	99.0	5.42
36	Diflunisal	91.8	52.9	47.6	39.0	0.0	32.5	2.67	98.7	5.15
37	Diltiazem	40.7	71.7	87.2	0.0	15.5	41.6	3.71	58.5	1.15
38	Diphenhydramine	40.0	59.9	98.0	0.0	38.2	44.6	4.14	55.4	1.09
39	Diprophylline	19.7	18.2	18.1	1.5	−0.1	−4.0	1.08	25.9	0.63
40	Dipyridamole	38.2	68.9	72.1	0.0	3.3	43.2	3.94	87.3	2.23
41	Doxepin	41.2	64.3	108.2	0.0	43.9	52.3	5.61	83.2	1.95
42	Droperidol	36.3	68.0	76.4	0.0	8.3	39.3	3.40	88.0	2.29
43	Encainide	33.0	48.2	93.6	0.0	45.3	41.9	3.74	48.8	0.97
44	Ethinyl Estradiol	76.9	76.3	77.4	0.6	1.2	46.8	4.52	97.2	4.10
45	Famotidine	10.7	23.5	25.1	0.0	1.7	15.7	1.62	14.5	0.46
46	Felbamate	64.7	63.6	65.8	1.1	2.2	24.6	2.08	68.7	1.39
47	Felodipine	98.7	99.4	99.5	0.0	0.1	46.1	4.39	95.5	3.46
48	Fenclofenac	90.4	55.5	47.7	35.0	0.0	35.6	2.98	98.8	5.23
49	Fenoprofen	83.4	48.7	42.7	34.7	0.0	26.3	2.19	99.3	5.91
50	Finasteride	75.9	73.2	75.9	2.7	2.7	38.9	3.35	74.7	1.58
51	Floxacillin	76.3	48.6	45.4	27.6	0.0	23.4	2.00	96.0	3.62
52	Flumazenil	49.0	48.5	50.3	0.0	1.7	18.4	1.74	20.9	0.56
53	Flunarizine	55.2	121.2	125.8	0.0	4.6	52.6	5.67	97.5	4.26
54	Flunitrazepam	71.0	71.1	72.3	0.0	1.2	31.2	2.56	79.7	1.77
55	Fluoxetine	48.1	67.5	107.3	0.0	39.8	52.9	5.73	97.1	4.01
56	Flurazepam	38.2	69.1	93.4	0.0	24.3	41.8	3.73	59.4	1.17
57	Flurbiprofen	85.5	47.5	44.8	38.0	0.0	26.8	2.22	100.0	7.81
58	Furosemide	32.4	−21.7	−31.7	54.1	0.0	−4.2	1.08	63.8	1.26
59	Gemfibrozil	51.6	79.7	49.3	0.0	0.0	32.9	2.71	96.1	3.64
60	Glipizide	67.9	46.0	38.9	21.9	0.0	21.1	1.87	95.0	3.32
61	Griseofulvin	71.4	70.9	72.5	0.5	1.6	33.1	2.73	72.1	1.49
62	Hexobarbital	63.5	63.3	30.7	0.2	0.0	18.8	1.76	27.7	0.66
63	Hydralazine	36.9	31.9	33.2	5.1	1.3	13.3	1.52	48.8	0.97
64	Hydrochlorothiazide	32.0	30.8	−30.9	1.2	0.0	15.9	1.63	35.6	0.77
65	Hydrocortisone	52.7	50.5	52.4	2.2	2.0	27.9	2.30	45.8	0.92
66	Imipramine	46.1	69.1	118.6	0.0	49.4	54.1	6.04	83.2	1.95
67	Indomethacin	88.6	54.0	48.5	34.7	0.0	32.5	2.68	99.5	6.17
68	Indoramin	35.2	52.2	71.1	0.0	18.9	1.9	3.74	72.1	1.49
69	Isradipine	89.0	89.8	90.4	−0.8	0.6	40.0	3.49	92.8	2.86
70	Ketoconazole	40.9	78.8	81.3	0.0	2.5	42.9	3.89	93.0	2.90
71	Ketoprofen	74.3	41.2	38.1	33.2	0.0	21.9	1.92	98.4	4.80
72	Labetalol	34.5	46.3	42.2	0.0	0.0	41.4	3.67	64.6	1.28
73	Levamisol	13.3	44.5	61.0	0.0	16.5	34.7	2.89	36.4	0.78

Table 1. Continued

No	drug	CHI pH 2.0	CHI pH 7.4	CHI pH 10.5	delta CHI neg chrg	delta CHI pos chrg	CHI IAM	log *K* (IAM)	HSA %	log *K* (HSA)
				(a) Training Set						
74	Levonorgestrel	85.6	85.0	85.8	0.6	0.9	41.2	3.65	93.4	2.98
75	Lignocaine	22.6	73.9	86.7	0.0	12.7	29.6	2.43	29.8	0.69
76	Lorazepam	64.6	63.9	65.4	0.7	1.6	37.3	3.16	91.1	2.62
77	Maprotiline	45.2	61.1	115.3	0.0	54.1	52.9	5.74	83.2	1.95
78	Mebendazole	48.2	61.0	59.8	0.0	0.0	37.5	3.19	89.8	2.46
79	Methyl-prednisolone	57.5	56.5	58.2	1.0	1.6	32.1	2.65	54.9	1.35
80	Metronidazole	8.5	21.0	22.4	0.0	1.5	−3.3	1.09	5.4	0.76
81	Mianserin	67.1	65.9	68.5	1.2	2.6	33.7	2.79	85.6	2.12
82	Minoxidil	23.1	33.7	35.9	0.0	2.2	19.0	1.77	27.9	0.66
83	*N*-Dealkyl-flurazepam	66.8	68.1	70.6	0.0	2.5	36.5	3.08	92.6	2.84
84	Nabumetone	87.9	88.7	89.4	0.0	0.7	38.4	3.29	94.3	3.16
85	Nadolol	19.4	25.9	45.2	0.0	19.3	20.2	1.83	16.5	0.49
86	Naproxen	75.2	40.2	36.1	35.0	0.0	22.9	1.97	99.9	7.06
87	Neostigmine	5.6	20.0	37.0	0.0	16.9	17.3	1.69	87.6	2.26
88	Nicardipine	46.3	101.1	103.9	0.0	2.8	45.9	4.35	93.2	2.93
89	Nifedipine	76.1	77.3	78.7	0.0	1.4	29.0	2.39	69.5	1.41
90	Nisoldipine	95.8	98.0	98.7	0.0	0.7	37.4	3.18	91.0	2.61
91	Nitrazepam	59.6	64.2	63.9	0.0	0.0	33.3	2.75	82.3	1.91
92	Nitrendipine	87.9	88.4	89.0	0.0	0.6	40.5	3.56	94.2	3.13
93	Nitrofurantoin	39.9	33.3	21.0	6.5	0.0	6.2	1.30	71.5	0.85
94	Nizatidine	5.6	29.9	33.6	0.0	3.8	17.9	1.72	20.4	0.55
95	Nordazepam	55.5	70.3	72.9	0.0	2.6	38.3	3.28	92.6	2.83
96	Nortriptyline	44.0	62.9	118.3	0.0	55.4	52.6	5.66	86.2	2.15
97	Ondansetron	31.7	51.8	60.3	0.0	8.4	37.2	3.15	77.7	1.69
98	Oxacillin	69.3	42.4	40.4	26.9	0.0	18.9	1.76	87.8	2.28
99	Oxazepam	62.3	62.0	63.7	0.4	1.7	36.2	3.04	94.2	3.12
100	Papaverine	32.6	65.8	68.0	0.0	2.2	34.4	2.86	88.6	2.35
101	Pentobarbital	62.0	59.3	31.3	2.7	0.0	22.4	1.95	28.8	0.67
102	Pentoxifylline	39.5	37.8	39.2	1.7	1.4	12.0	1.48	25.9	0.63
103	Perphenazine	38.8	76.0	93.7	0.0	17.7	56.3	6.60	94.8	3.27
104	Phenytoin	61.0	60.6	37.3	0.4	0.0	31.6	2.59	75.5	1.60
105	Pindolol	20.9	31.5	56.7	0.0	25.2	30.3	2.49	19.7	0.54
106	Piperacillin	40.0	35.1	33.1	4.8	0.0	9.4	1.39	15.4	0.48
107	Piroxicam	19.8	33.6	35.0	0.0	1.4	6.8	1.31	97.7	4.36
108	Prazosin	30.1	48.7	52.9	0.0	4.2	31.6	2.60	80.4	1.81
119	Prednisolone	51.9	49.5	51.5	2.4	2.0	28.0	2.31	43.6	0.89
110	Prednisone	52.2	51.4	53.2	0.8	1.8	25.9	2.16	37.6	0.80
111	Primidone	37.7	36.1	36.9	1.6	0.8	8.9	1.37	25.3	0.62
112	Probenecid	79.8	47.4	44.0	32.5	0.0	20.1	1.82	95.4	3.44
113	Procainamide	−34.8	16.6	41.7	0.0	25.1	19.9	1.81	35.2	0.76
114	Procyclidine	91.3	90.9	89.3	0.4	0.0	46.7	4.49	96.5	3.77
115	Propranolol	37.0	50.3	83.0	0.0	32.7	45.1	4.23	66.5	1.33
116	Propylthiouracil	30.1	28.0	8.2	2.1	0.0	3.9	1.24	33.1	0.73
117	Protryptyline	43.4	60.6	117.4	0.0	56.7	51.6	5.45	83.8	1.99
118	Proxyphylline	26.5	24.9	25.4	1.6	0.5	1.1	1.17	25.9	0.63
119	Quinidine	14.6	46.4	71.2	0.0	24.8	45.0	4.20	77.0	1.66
120	Quinine	16.3	46.7	69.4	0.0	22.7	47.1	4.56	76.7	1.65
121	Ranitidine	8.9	23.7	41.7	0.0	18.0	28.0	2.31	17.5	0.51
122	Sulfachlor-pyridazine	45.7	23.2	17.5	22.5	0.0	6.0	1.29	91.5	2.67
123	Sulfameter	39.0	28.2	−26.1	10.8	0.0	3.7	1.23	83.5	1.97
124	Sulfamethoxypyridazine	36.0	33.8	14.4	2.1	0.0	9.6	1.40	84.5	2.04
125	Sulfametopyrazine	43.4	22.3	−22.7	21.1	0.0	−0.4	1.14	68.9	1.39
126	Sulfapyridine	23.5	29.9	15.4	0.0	0.0	11.4	1.46	18.8	0.53
127	Sulfinpyrazone	77.6	47.8	44.0	29.8	0.0	26.1	2.17	97.2	4.09
128	Sulfisoxazole	51.7	19.5	14.8	32.2	0.0	2.9	1.21	88.4	2.33
129	Sulphadimethoxine	56.1	38.4	18.9	17.8	0.0	10.8	1.44	94.4	3.17
130	Sulphadimidine	31.7	35.6	19.1	0.0	0.0	10.6	1.43	73.6	1.54
131	Sulpiride	9.3	23.2	48.2	0.0	25.0	25.5	2.14	34.3	0.75
132	Tamoxifen	58.6	107.9	137.2	0.0	29.3	58.7	7.29	98.4	4.84
133	Temazepam	70.9	71.0	73.0	0.0	1.9	34.7	2.89	94.9	3.28
134	Terbutaline	8.8	15.8	18.7	0.0	2.9	16.8	1.67	28.8	0.67
135	Theobromine	14.6	13.1	7.0	1.5	0.0	−4.1	1.08	64.8	1.29
136	Tinidazole	33.3	35.6	35.8	0.0	0.2	0.4	1.16	25.9	0.63
137	Tolbutamide	71.8	46.0	35.3	25.8	0.0	10.2	1.42	96.0	3.59
138	Tolfenamic Acid	100.7	61.1	52.8	39.6	0.0	41.9	3.74	98.2	4.68
139	Tolmetin	71.7	41.5	38.9	30.2	0.0	20.9	1.87	96.5	3.77
140	Tramadol	27.0	41.2	86.4	0.0	45.2	28.9	2.38	25.3	0.62
141	Trazodone	34.8	70.9	75.6	0.0	4.8	36.3	3.05	89.8	2.46
142	Trimethoprim	21.1	37.1	40.4	0.0	3.4	20.8	1.86	39.5	0.80
143	Viloxazine	27.8	42.2	55.4	0.0	13.2	31.1	2.56	20.9	0.56
144	Vinblastine	33.8	82.6	93.7	0.0	11.0	50.4	5.19	81.7	1.87
145	Vincristine	31.9	74.1	84.5	0.0	10.3	47.7	4.67	74.1	1.55
146	Warfarin	81.5	45.7	34.1	35.8	0.0	19.9	1.81	97.9	4.45
147	Zidovudine	31.6	30.1	22.5	1.5	0.0	1.3	1.18	12.8	0.43

Table 1. Continued

No	drug	CHI pH 2.0	CHI pH 7.4	CHI pH 10.5	delta CHI neg chrg	delta CHI pos chrg	CHI IAM	log *K* (IAM)	HSA %	log *K* (HSA)
					(a) Training Set					
148	Zolmitriptan	18.1	26.6	49.8	0.0	23.2	29.7	2.44	30.6	0.70
149	Zolpidem	32.0	63.4	66.1	0.0	2.7	33.9	2.81	73.6	1.54
					(b) Test Set					
1	Acyclovir	−28.4	−22.5	−32.7	0.0	0.0	−7.0	1.03	5.4	0.29
2	Aminoglutethimide	14.9	45.4	47.1	0.0	1.7	16.0	1.63	18.9	0.53
3	Antipyrine	33.8	34.0	36.3	0.0	2.3	9.7	1.40	12.8	0.43
4	Ceftazidime	15.0	11.1	8.1	4.0	0.0	−5.1	1.06	7.9	0.34
5	Chlor-phentermine	47.8	81.2	82.8	0.0	1.7	44.1	4.06	94.0	3.08
6	Cimetidine	10.4	26.2	30.5	0.0	4.2	16.6	1.66	21.2	0.56
7	Daunorubicin	40.4	50.5	61.5	0.0	11.0	50.7	5.25	77.1	1.66
8	Dexa-methasone	60.4	59.1	60.4	1.3	1.4	31.3	2.57	70.9	1.45
9	Dicloxacillin	79.6	50.4	47.8	29.2	0.0	27.4	2.26	95.7	3.50
10	Domperidone	35.2	55.1	64.9	0.0	9.7	41.9	3.74	91.2	2.64
11	Dothiepin	43.6	40.4	112.4	0.0	72.0	52.1	5.57	87.8	2.28
12	Flunisolide	65.6	63.3	65.0	2.4	1.8	32.1	2.64	39.0	0.82
13	Ganciclovir	−36.3	−22.3	−34.1	0.0	0.0	−12	0.97	12.8	0.43
14	Glyburide	86.8	68.4	52.2	18.4	0.0	34.5	2.86	98.0	4.51
15	Haloperidol	41.9	62.7	88.4	0.0	25.7	45.2	4.24	81.1	1.84
16	Ibuprofen	91.8	51.4	44.7	40.4	0.0	22.8	1.97	99.6	6.28
17	Indoprofen	65.7	36.9	34.8	28.8	0.0	20.5	1.85	98.0	4.55
18	Mephobarbital	65.6	64.2	29.5	1.4	0.0	22.2	1.93	37.0	0.79
19	Meto-clopramide	25.1	36.6	65.4	0.0	28.8	35.4	2.95	51.4	1.02
20	Nimodipine	52.7	52.3	54.0	0.5	1.8	29.0	2.39	81.4	1.86
21	Phenacetin	51.7	50.7	52.1	1.0	1.3	18.9	1.76	35.2	0.76
22	Phenobarbital	51.6	49.4	18.4	2.3	0.0	13.6	1.53	35.2	0.76
23	Phenylbutazone	81.5	51.5	41.4	30.1	0.0	25.7	2.15	98.4	4.82
24	Propafenone	44.9	90.5	99.7	0.0	9.2	42.3	3.80	91.1	2.62
25	Pyrimethamine	34.2	57.8	63.6	0.0	5.9	37.0	3.13	85.9	2.13
26	Rifampin	61.3	61.2	58.4	0.1	0.0	36.0	3.02	77.2	1.67
27	Saquinavir	48.9	89.7	92.6	0.0	2.8	43.5	3.97	95.2	3.38
28	Tetroxoprim	23.2	37.6	41.7	0.0	4.1	20.9	1.86	23.7	0.60
29	Vancomycin	14.2	20.0	18.9	0.0	0.0	21.6	1.90	38.8	0.82
30	Verapamil	44.4	72.0	100.2	0.0	28.1	42.0	3.75	77.9	1.70

[a] CHI, chromatographic hydrophobicity index; delta CHI neg chrg and pos chrg, the differences of the CHI values obtained at pH 2 and pH 7.4 and at pH 10.5 and 7.4, respectively; Negative values were taken as zero; CHI IAM, chromatographic hydrophobicity index obtained on IAM column; log *K* (IAM), the logarithm of the compounds partition coefficient into IAM derived from CHI IAM; HSA %, the % binding to HSA obtained from the retention times on HSA HPLC columns; log *K* (HSA), the logarithm of the association constant of HSA binding derived also from the HPLC retention times.

high; the compound eluted only on the isocratic region of the 70% acetonitrile mobile phase, giving a log *K* (IAM) value of 9.89. On the basis of these values, the estimated VD of Amiodarone would be over 300 L/kg. For the correct estimation of compounds with this extreme large volume data, we need to apply a longer gradient method for the measurement of IAM binding. Also, Amiodarione could not be eluted from the C-18 columns either, because of its high lipophilicity.

A further improvement in the model was obtained; by using the deltaCHI values, we account for the presence of the positive and negative charges. This is described by eq 7.

$$\text{Log VD} = 0.33(\pm 0.03)\log K\,(\text{IAM}) - 0.11(\pm 0.03)\log K\,(\text{HSA}) - 0.016(\pm 0.003)\,\Delta\text{CHInegchrg} + 0.005(\pm 0.002)\Delta\text{CHIposchrg} - 0.52 \quad (7)$$

where $N = 179$, $r^2 = 0.79$, $s = 0.31$, and $F = 168$.

This additional influence of charge may account for the permeability barriers and pH differences caused by charges when compounds cross biological compartments.

The predominant charge state of the compounds at physiological pH (pH 7.4) was also assigned based on the calculated pK_a values of the compounds, as is shown in Table 2 and explained in the Experimental Section.

When acid/base class descriptors based on calculated pK_a values were introduced into the model instead of delta CHI charge descriptors, eq 8 was obtained and shows similar statistics to eq 7.

$$\text{Log VD} = 0.30(\pm 0.03)\log K\,(\text{IAM}) - 0.12(\pm 0.02)\log K\,(\text{HSA}) - 0.08(\pm 0.01)\,\text{p}K_a\ \text{acid class} + 0.02(\pm 0.01)\,\text{p}K_a\ \text{base class} - 0.45 \quad (8)$$

where $N = 179$, $r^2 = 0.80$, $s = 0.30$, and $F = 177$.

For comparison, we constructed a model using only in silico parameters, namely, the calculated lipophilicity (*c* log *P*) and parameters that describe the charge state of the molecules based on calculated pK_a values. Equation 9 describes the model, which was obtained and explains reasonably the variation of the VD_{ss}.

$$\text{Log VD} = 0.085(\pm 0.02)c\log P - 0.141(\pm 0.011)\,\text{p}K_a\ \text{acid class} + 0.078(\pm 0.012)\,\text{p}K_a\ \text{base class} - 0.089 \quad (9)$$

where $N = 179$, $r^2 = 0.68$, $s = 0.38$, and $F = 125$.

Figure 4 shows the measured versus the predicted log VD values obtained by eq 9.

It can be seen that, although a reasonable model can be constructed, the predictive power of this model was significantly poorer when compared with eq 7 or 8.

Statistical Analysis of the Models Obtained. All the predictor variables in the equations are statistically significant at the $p < 0.0001$ level.

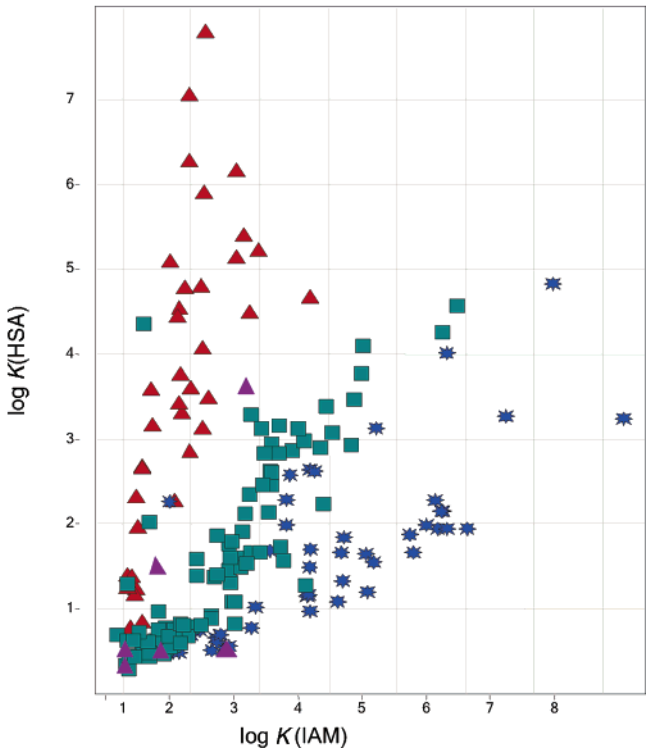

Figure 2. Effect of the positive and negative charges on the compounds' binding to IAM and HSA. Legend: acid (red triangle); base (star); neutral (square); zwitterions (purple triangle).

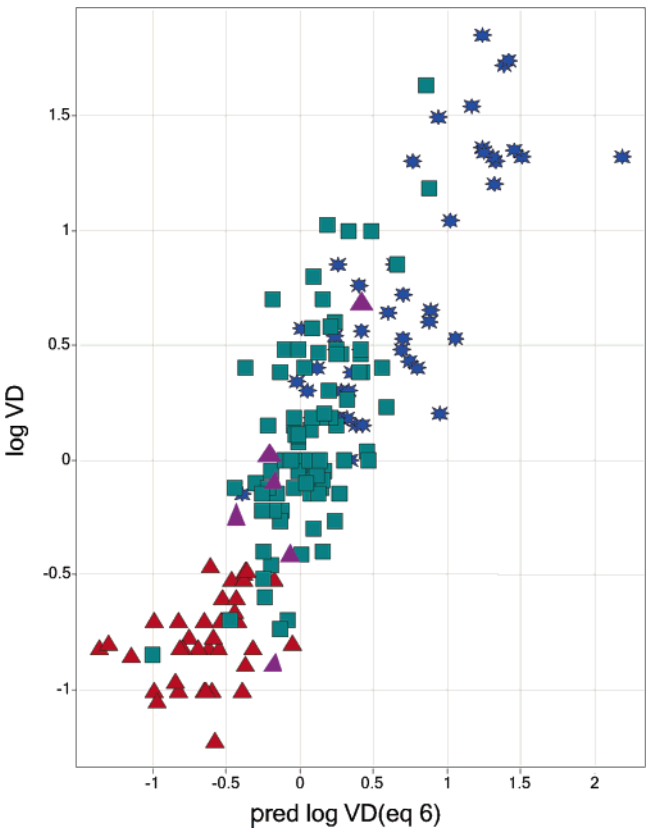

Figure 3. The plot of the literature vs predicted log VD values for 179 compounds based on eq 6. Legend: acid (red triangle); base (star); neutral (square); zwitterions (purple triangle).

To further explore the predictive power and ruggedness of the actual model, the whole data set was subdivided into a training set and a test set. The statistical parameters obtained are summarized in Table 3.

Table 2. Determination of the Number of Charge State Groups with the Help of Predicted pK_a Values in Acid/Base Classes

charge state group	acid class	base class
0	no acidic group	no basic group
1	pK_a > 8.5	pK_a ≤ 6.0
2	pK_a 7.5 − 8.5	pK_a 6.0 − 7.0
3	pK_a 7.0 − 7.49	pK_a 7.01 − 7.5
4	pK_a 6.5 − 6.99	pK_a 7.51 − 8.0
5	pK_a 6.0 − 6.49	pK_a 8.01 − 8.5
6	pK_a 5.5 − 5.99	pK_a 8.51 − 9.0
7	pK_a < 5.5	pK_a > 9.0

The calculated VD values for the test set are summarized in Table 4 and visualized in Figure 5.

The mean fold error of the predictions was calculated from the equations obtained. The mean fold error for eqs 6−8 was found to be around 1.3 (1.285, 1.278, and 1.289, respectively). Mean fold error following prediction via eq 9 using in silico parameters was slightly higher, with a value of 1.469.

The fold error columns are shown in Table 4 and represent the fold error of the calculations for eqs 6−9.

In a previous study, where only basic and neutral compounds were investigated, the mean fold error was calculated to be 2.26.[44] However, the ratio of compounds in the test series to those in the training set was different (18:120). In comparison with the error normally associated with the prediction using interspecies scaling, which is reported to be in the range of 1.56−2.78,[19,20] our mean fold errors are encouraging.

Comparison of our Models with Other Published Models. We were also interested in testing our models using external data. A data set of 120 compounds, published by Lombardo and co-workers,[46] offered a good opportunity to compare our models, because 41 compounds (17 bases and 24 neutrals) were common to the two databases. The calculated VD data based on our models and based on the model by Lombardo et al.[44]

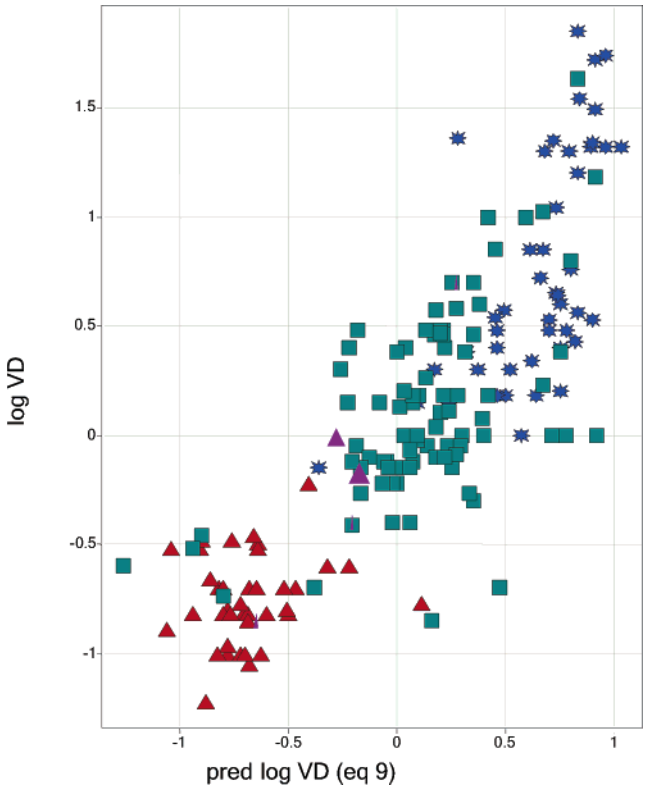

Figure 4. The plot of the literature vs in silico predicted log VD values for 179 compounds obtained by eq 9. Legend: acid (red triangle); base (star); neutral (square); zwitterions (purple triangle).

Table 3. Statistical Characteristics of the Models Obtained for the Training Set and Test Set

		training set				test set			
eq No	equation	*N*	R^2	RMSE	*F*	*N*	R^2	RMSE	*F*
6	0.43log *K* (IAM) − 0.23log *K* (HSA) − 0.65	149	0.75	0.33	218	30	0.69	0.40	62
7	0.33log *K* (IAM) − 0.12log *K* (HSA) + 0.003deltaCHIpos − 0.016deltaCHIneg − 0.51	149	0.80	0.31	140	30	0.73	0.37	76
8	0.30log *K* (IAM) − 0.11log *K* (HSA) + 0.022pK_a base class − 0.08pK_a acid class − 0.45	149	0.82	0.29	164	30	0.72	0.38	71
9	0.10*c* log *P* + 0.07pK_a base class − 0.14pK_a acid class − 0.11	149	0.72	0.36	122	30	0.51	0.50	29

Table 4. The Literature and Predicted VD Data and the Fold Error Obtained by eq 6 - to 9 for the Test Set of Compounds

No	drug	log VD obs	log VD calc eq 6	log VD calc eq 7	log VD calc eq 8	log VD calc eq 9	fold error eq 6	fold error eq 7	fold error eq 8	fold error eq 9
1	Acyclovir	−0.16	−0.28	−0.21	−0.16	−0.27	1.34	1.16	1.02	1.34
2	Amino-glutethimide	0.15	−0.07	−0.04	−0.08	−0.10	1.66	1.53	1.69	1.76
3	Antipyrine	−0.22	−0.15	−0.10	−0.06	−0.01	1.18	1.32	1.45	1.62
4	Ceftazidime	−0.64	−0.28	−0.27	−0.73	−1.36	1.23	1.25	2.31	9.88
5	Chlorphentermine	0.38	0.39	0.45	0.59	0.69	1.02	1.17	1.63	2.03
6	Cimetidine	0.00	−0.07	−0.03	0.03	0.07	1.18	1.06	1.06	1.19
7	Daunorubicin	1.36	1.22	1.05	1.01	0.19	1.39	2.07	2.27	14.71
8	Dexamethasone	−0.09	0.12	0.14	0.16	0.07	1.20	1.24	1.31	1.07
9	Dicloxacillin	−0.07	−0.47	−0.66	−0.71	−0.74	3.77	2.42	2.15	2.02
10	Domperidone	0.76	0.35	0.42	0.52	0.76	2.52	2.15	1.72	1.00
11	Dothiepin	1.85	1.21	1.26	1.12	0.78	4.28	3.82	5.36	11.55
12	Flunisolide	0.26	0.29	0.22	0.25	0.13	1.09	1.08	1.01	1.32
13	Ganciclovir	0.04	−0.33	−0.25	−0.19	−0.29	1.51	1.24	1.09	1.35
14	Glyburide	−0.52	−0.44	−0.42	−0.66	−0.69	2.60	2.73	1.55	1.47
15	Haloperidol	1.26	0.74	0.73	0.74	0.64	3.24	3.32	3.30	4.11
16	Ibuprofen	−0.82	−1.22	−1.28	−1.13	−0.74	2.48	2.86	2.04	1.21
17	Indoprofen	−1.00	−0.88	−0.92	−0.96	−0.76	1.31	1.19	1.10	1.72
18	Mepho-barbital	0.40	0.00	0.00	0.04	0.05	2.52	2.48	2.28	2.24
19	Metoclopramide	0.53	0.38	0.42	0.48	0.63	1.41	1.28	1.12	1.24
20	Nimodipine	−0.05	−0.05	0.04	0.06	0.31	1.68	1.37	1.31	1.35
21	Phenacetin	0.18	−0.07	−0.04	−0.01	0.07	1.77	1.64	1.53	1.28
22	Pheno-barbital	−0.27	−0.17	−0.14	−0.16	−0.18	1.08	1.15	1.10	1.04
23	Phenyl-butazone	−0.77	−0.81	−0.88	−0.42	0.11	1.11	1.28	2.22	7.64
24	Propafenone	0.56	0.38	0.44	0.56	0.77	1.49	1.30	1.02	1.62
25	Pyrimethamine	0.46	0.21	0.27	0.30	0.34	3.74	4.35	4.64	5.07
26	Rifampin	−0.01	0.26	0.27	0.35	0.64	4.83	4.93	5.88	11.38
27	Saquinavir	1.00	0.28	0.38	0.44	0.58	5.20	4.13	3.63	2.61
28	Tetroxoprim	−0.10	0.01	0.04	0.11	0.19	1.28	1.36	1.60	1.92
29	Vancomycin	−0.41	−0.02	0.01	0.03	−0.22	2.43	2.63	2.73	1.55
30	Verapamil	0.64	0.57	0.60	0.61	0.70	1.27	1.18	1.17	1.07
	Mean fold error						2.09	2.02	2.08	3.31

are listed in Table 5. The comparison of the observed and predicted VD values by our models and Lombardo's model were very similar. Mean fold error values of predictions based on our models were slightly better for the overlapping data set than that obtained for our whole dataset with 179 compounds. Also the correlation between the measured and observed values by our models ($r^2 = 0.58 - 0.60$; except eq 9) were similar to that obtained for Lombardo's model for the overlapping 42 compounds ($r^2 = 0.60$).

To examine the application of our model in daily practice, we applied our measurements and the equations for new research compounds.

A comparison of the in-house measured and calculated VD in rats for 247 new research compounds from several projects studied at GlaxoSmithKline showed a very similar scatter plot and cluster formation according to their acid/base character as we observed in the case of known drug molecules on human data.

Figure 6 shows the plots of the predicted versus the observed log VD data for new research compounds compared to the

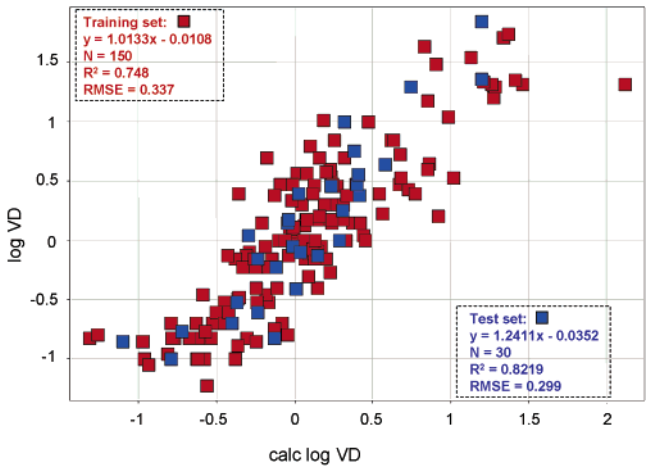

Figure 5. The plot of the literature vs predicted log VD values for 149 training set compounds and for 30 test set compounds based on eq 6.

Table 5. Comparison of the Observed and Calculated VD Data for the 41 Overlapping Drug Molecules[a]

No	drug	log VD obs	calc log VD[a]	calc log VD eq 6	calc log VD eq 7	calc log VD eq 8	calc log VD eq 9	fold error eq 6	fold error eq 7	fold error eq 8	fold error eq 9
1	Antipyrine	−0.22	−0.20	−0.15	−0.10	−0.06	−0.01	1.18	1.32	1.45	1.62
2	Beta-methasone	0.15	0.11	0.22	0.18	0.21	0.07	1.27	1.18	1.25	1.10
3	Bromazepam	−0.05	−0.08	0.04	0.09	0.12	0.14	1.20	1.36	1.45	1.50
4	Chlor-pheniramine	0.51	0.80	1.03	0.98	0.93	0.64	3.38	2.99	2.69	1.38
5	Cimetidine	0.00	−0.01	−0.07	−0.03	0.03	0.07	1.18	1.06	1.06	1.19
6	Clonidine	0.32	0.42	0.21	0.24	0.30	0.40	1.29	1.20	1.05	1.20
7	Colchicine	0.13	−0.14	0.03	0.03	0.07	0.01	4.81	4.85	4.46	5.05
8	Dexa-methasone	0.09	0.04	0.12	0.14	0.16	0.07	1.20	1.24	1.31	1.07
9	Diazepam	0.04	0.10	0.05	0.17	0.20	0.28	1.17	1.15	1.23	1.47
10	Diphen-hydramine	0.65	0.74	0.87	0.83	0.81	0.68	1.65	1.52	1.44	1.07
11	Domperidone	0.76	0.89	0.35	0.42	0.52	0.76	2.52	2.15	1.72	1.00
12	Felodipine	1.00	0.36	0.45	0.51	0.49	0.45	3.57	3.12	3.22	3.55
13	Flumazenil	0.02	−0.17	−0.04	−0.01	0.03	0.08	1.19	1.12	1.03	1.08
14	Haloperidol	1.26	0.90	0.74	0.73	0.74	0.64	3.24	3.32	3.30	4.11
15	Hydro-cortisone	0.40	−0.13	0.13	0.10	0.14	0.06	3.04	2.88	3.13	2.63
16	Labetalol	0.97	0.39	0.63	0.54	0.51	0.37	1.13	1.39	1.49	2.07
17	Lorazepam	0.18	0.13	0.11	0.20	0.23	0.20	1.24	1.01	1.07	1.00
18	Maprotiline	1.72	0.87	1.36	1.31	1.23	0.85	1.86	2.12	2.54	6.01
19	Methylprednisolone	0.08	0.10	0.24	0.21	0.22	0.07	1.23	1.17	1.20	1.20
20	Meto-clopramide	0.53	0.65	0.38	0.42	0.48	0.63	1.41	1.28	1.12	1.24
21	Metronidazole	−0.13	−0.24	−0.25	−0.19	−0.14	−0.08	1.32	1.14	1.02	1.13
22	Nadolol	0.30	0.34	0.02	0.09	0.20	0.44	1.82	1.56	1.20	1.46
23	Nifedipine	−0.11	0.11	0.05	0.10	0.13	0.31	1.44	1.62	1.74	2.59
24	Nizatidine	0.08	−0.17	−0.04	−0.01	0.14	0.31	1.33	1.22	1.14	1.71
25	Nortriptyline	1.36	0.84	1.28	1.26	1.18	0.83	1.01	1.05	1.26	2.80
26	Oxazepam	−0.22	0.13	−0.05	0.10	0.14	0.20	1.50	2.14	2.35	2.66
27	Pentoxifylline	0.38	−0.21	−0.16	−0.13	−0.06	−0.02	6.11	5.65	4.81	4.41
28	Perphenazine	1.35	1.13	1.43	1.31	1.30	0.69	1.35	1.02	1.01	4.11
29	Pindolol	0.36	0.45	0.29	0.32	0.40	0.57	1.02	1.04	1.24	1.86
30	Prednisolone	0.18	−0.12	0.14	0.10	0.14	0.04	2.63	2.45	2.68	2.09
31	Prednisone	−0.01	−0.13	0.09	0.09	0.11	0.06	1.27	1.27	1.32	1.18
32	Procainamide	0.28	0.38	−0.05	0.07	0.16	0.55	2.12	1.63	1.30	1.85
33	Propafenone	0.56	0.70	0.38	0.44	0.56	0.77	1.49	1.30	1.02	1.62
34	Propranolol	0.63	0.61	0.85	0.82	0.84	0.68	1.79	1.64	1.72	1.19
35	Quinidine	0.43	0.59	0.77	0.74	0.79	0.68	1.68	1.58	1.77	1.37
36	Ranitidine	0.11	0.34	0.22	0.24	0.32	0.39	1.28	1.34	1.61	1.90
37	Terbutaline	0.20	0.16	−0.09	−0.04	0.05	0.31	2.22	1.97	1.61	1.13
38	Trazodone	0.00	0.33	0.10	0.20	0.35	0.72	1.26	1.59	2.25	5.24
39	Trimethoprim	0.26	0.13	−0.04	0.01	0.08	0.21	1.76	1.58	1.33	1.01
40	Verapamil	0.64	0.89	0.57	0.60	0.61	0.70	1.27	1.18	1.17	1.07
41	Zidovudine	0.15	−0.25	−0.25	−0.20	−0.23	−0.24	2.99	2.72	2.90	2.99
	Mean fold error							1.89	1.81	1.80	2.10

[a] Published by Lombardo et al. (43).

known drug molecules in training set for human data. It can be seen that the human model works reasonably well to estimate VD in rats as well. Though our aim was to model directly the human VD, we have fitted an equation for the rat VD data as well for the "in-house" research compounds:

$$\log \mathrm{VD} = 0.27 \log K\,(\mathrm{IAM}) - 0.29 \log K\,(\mathrm{HSA}) - 0.30 \quad (10)$$

where $n = 247$, $r^2 = 0.66$, $s = 0.35$, and $F = 234$.

From the comparison of the regression coefficients of eqs 6 and 10, we can conclude that the tissue/plasma ratio is different in rats and humans, so allometric scaling should be applied when rat data are extrapolated to human data. The fact that our measured membrane partitioning [log *K* (IAM)] and HSA binding [log *K* (HSA)] parameters sufficiently can describe the rat VD suggests that our mechanistic approach was correct when we assumed that the VD can be considered as the manifestation of the difference between the tissue and plasma partitioning of the compounds.

Qualitative Picture. The presence of charged functions within molecules has a major impact on their VD. In general, acidic compounds have the smallest VD and basic compounds have the largest VD (see Figure 3). Similarly, acidic compounds bind more strongly to HSA, while basic compounds bind more strongly to phospholipid membranes (see Figure 2).

Binding affinities of drugs to plasma proteins and tissue components are also dependent on lipophilicity; both are high for highly hydrophobic compounds.

These rough guidelines can be formulated to express how the relative magnitude of VD depends upon the ionization state at pH 7.4 and lipophilicity. However, we can expect deviations from these general rules if a compound binds exceptionally strongly to any other tissue and/or plasma components that are present in a lower concentration.

Conclusion

The VD in humans for 179 known drug molecules have been estimated successfully using the previously published high throughput HPLC based measurements of HSA binding and artificial membrane partition data.

The model is based on the premise that the extent of VD depends on the difference between the tissue partition and the plasma partition of a compound. The data supports the assumption that the difference between the tissue and plasma partition is dominated by the different binding strength of a compound to phospholipid membrane and serum albumin.

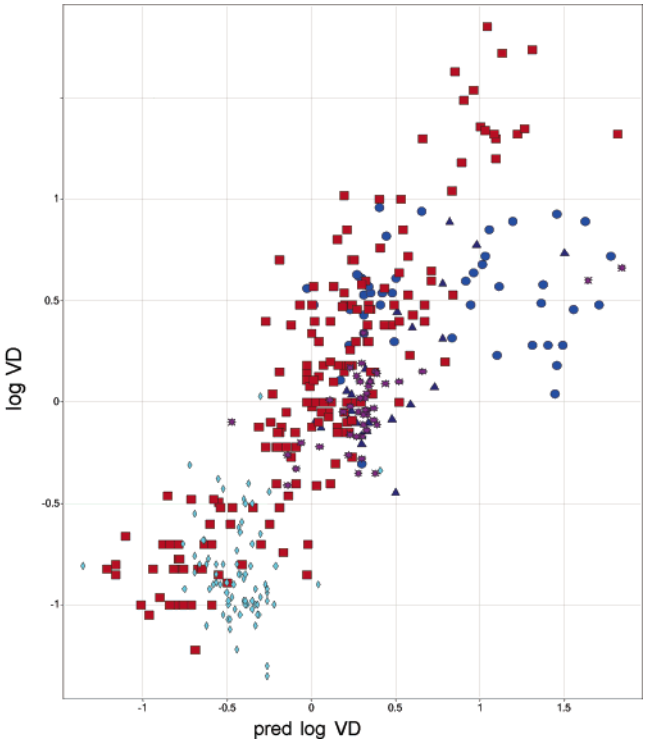

Figure 6. Application of model eq 6 for predicting log VD values of project compounds. The plot of the in house measured in rats vs predicted log VD values for project compounds. Legend: training set, 150 compounds, of the human log VD model (square); project 1 (diamond); project 2 (star); project 3 (triangle); project 4 (circle).

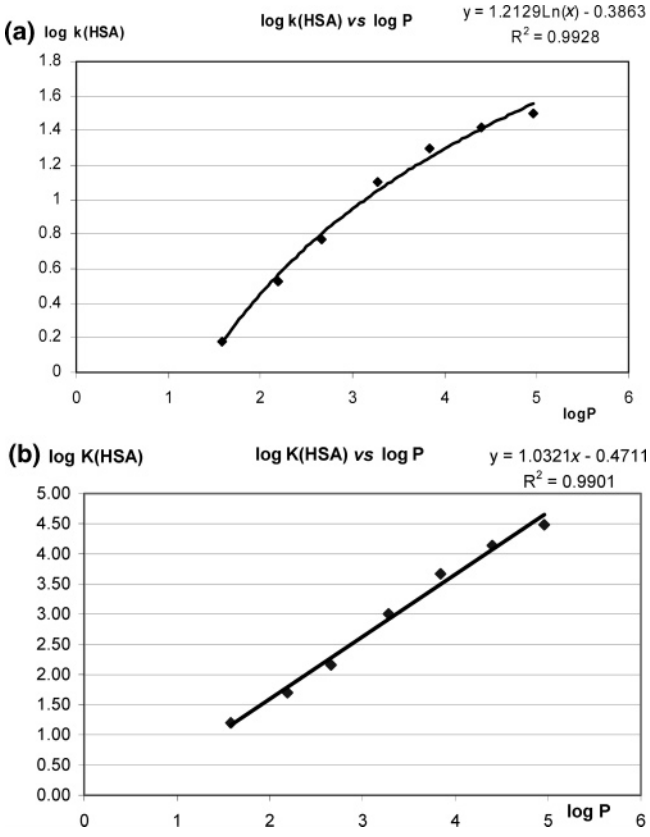

Figure 7. (a) The relationship of log *k* (HSA) to log *P* (octanol/water) for the acetophenone homologuous series. (b) The relationship of log *K* (HSA) to log *P* (octanol/water) for the acetophenone homologous series.

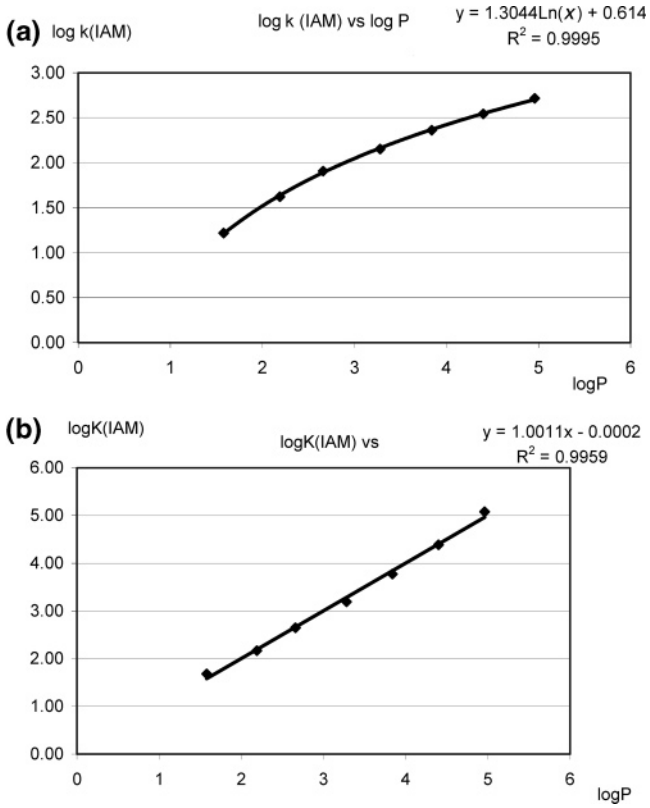

Figure 8. (a) The relationships of the log *k* (IAM) values to log *P* (octanol/water) for the acetophenone homologous series. (b) The relationships of the log *K* (IAM) values to log *P* (octanol/water) for the acetophenone homologous series.

It has been shown that in addition to a compound's lipophilicity, the presence of positive or negative charges at physiological pHs significantly affects the serum albumin binding and membrane partition and hence the VD.

It has been demonstrated that using the high throughput HPLC based biomimetic binding measurements (serum albumin binding and artificial membrane partition) on early drug discovery compounds their in vivo disposition can be estimated successfully. The application of these models helps to reduce the number of animal experiments. Also, it helps the compound design process, as chemists can be advised to modify the albumin binding and membrane partition data to tune the desired VD.

Experimental Section

VD and PPB data for 179 compounds were obtained from the scientific literature after an extensive comparative search. The data and the reference sources are compiled in Table 1a,b in Supporting Information. The compounds investigated in this study were all available commercially and selected to cover a wide variety of chemical structures, solute properties, pharmacological activities, and PK characteristics. In cases where the VD data were given for the whole body volume in liters, an average body weight of 70 kg for each study subject was assumed, and the VD_{ss} was expressed as L/kg.

Sample Preparation. Each compound was dissolved individually in DMSO (analytical grade, Fisher Scientific, Loughborough, U.K.) at a concentration of 10 mM. The 10 mM DMSO solutions then were diluted down 20 times with a mixture of 50% ammonium acetate buffer and 50% 2-propanol to ensure maximum dissolution, and 5 μL aliquots of the solutions were injected onto the HPLC columns.

Chromatographic System. Agilent HP1100 HPLC instruments equipped with diode array UV absorption detectors (Agilent

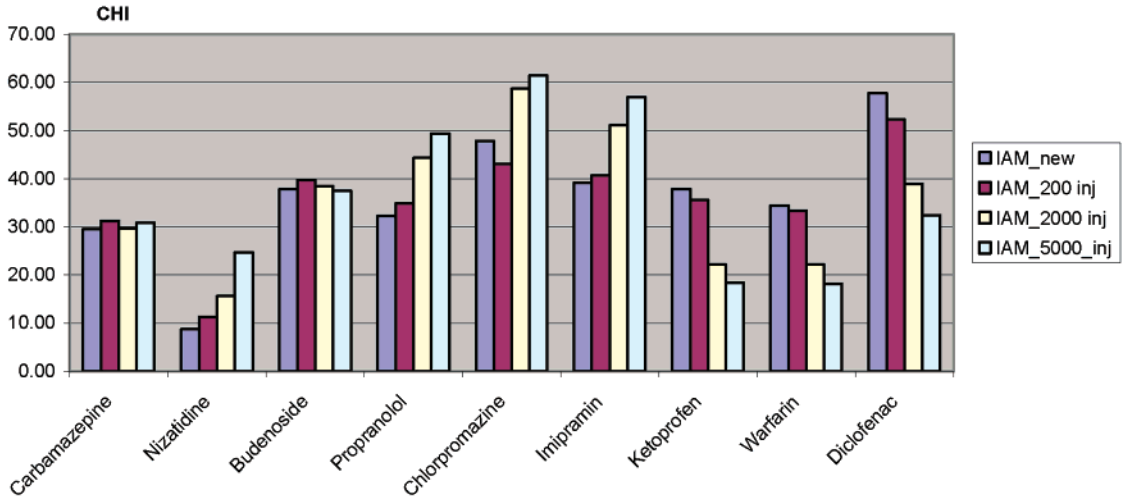

Figure 9. Reproducibility of the IAM HPLC column. Acids tend to give lower retention and bases longer retention as the column is aging.

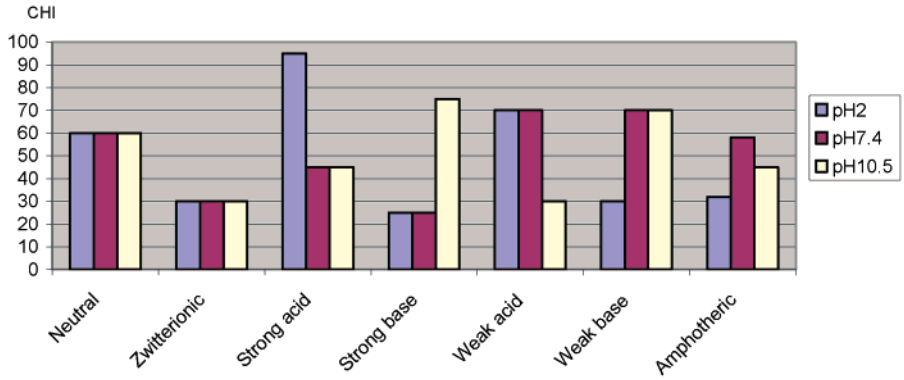

Figure 10. The CHI values at three different pHs for neutral, acidic, basic, amphoteric, and zwitterionic compounds.

HP1100) were used throughout. In all cases, chromatograms were recorded by HP Chemstation program at 230 and 254 nm.

HSA Binding Measurements. Chemically bonded HSA columns, with the dimensions of 50 mm × 3 mm id were obtained from Chromtech, Ltd (U.K.).

Mobile phase flow rate was 1.8 mL/min. The starting mobile phase was 50 mM aqueous ammonium acetate, with the pH adjusted to 7.4. Mobile phase B was 100% 2-propanol (HPLC grade). The gradient retention times of the compounds were recorded using the following gradient profile: 0 to 3 min linear gradient from 0 to 30% 2-propanol; 3 to 6 min constant mobile phase composition of 30% 2-propanol; 6 to 6.5 min linear gradient back to 0% 2-propanol (100% ammonium acetate buffer); and 6.5 to 10 min 100% ammonium acetate buffer.

The HSA column retention characteristics were calibrated with 10 known drug molecules (Warfarin, Nizatidine, Bromazepam, Carbamazepine, Budesonide, Piroxicam, Nicardipine, Ketoprofen, Indometacine, and Diclofenac), as described previously,[72] using literature % PPB data. The slope and the intercept of the logarithm of gradient retention time versus log K × PPB calibration line was used to estimate the log K (HSA) values from the log t_R values of the measured compounds.

It was found that the log k (HSA) values for the acetophenone homologues did not show a linear relationship with the log P values as it could have been expected from the theory derived for isocratic HPLC elution, see Figure 7a. The explanation for this is the application of the 2-propanol gradient. To scale the log k (HSA) values to other linear free energy related parameters such as log P (octanol/water partition coefficients) or log k_{aff} constants to the target receptor, we have taken the exponential value of the log k (HSA). We express it as log K (HSA) to be able to differentiate it from the previously published log k (HSA) data. The exponential function compensates for the effect of the gradient, that is, the constant change of the mobile phase composition during the binding measurements. The obtained log K (HSA) values show a linear relationship with the log P values for the acetophenone series, as is shown in Figure 7b.

To obtain log K (HSA) values from chromatographic retention data, the following mathematical transformation was made: Calculate log t_R from t_R, then convert log t_R to log k using the slope and intercept of the calibration line (log k = slope × log t_R + intercept), then calculate log K as log $K = e^{\log k}$. The literature PPB data were converted into log K × PPB, as described earlier.[72]

Phospholipid Binding Measurements. The binding measurements were carried out using IAM column (IAM PC2 S-12-300-IAM-PC), with the dimensions of 150 × 4.6 mm obtained from Regis (Morton Grove, U.S.A.), as described previously.[71] This stationary phase is composed of chemically bonded phosphatidyl choline (double acyl chain and glycerol backbone). Acetonitrile gradient was applied with the 50 mM ammonium acetate buffer, using 2 mL/min mobile phase flow rate. The following gradient profile was used: 0 to 2.5 min linear gradient from 0 to 70% acetonitrile; 2.5 to 3 min 70% acetonitrile; 3 to 3.2 min 70 to 0% acetonitrile; and 3.2 to 5 min re-equilibration with 100% 50 mM ammonium acetate buffer (pH 7.4).

The chromatographic hydrophobicity index values on the IAM column (CHI(IAM)) were obtained using the data for the calibration standards obtained from isocratic measurements, as described previously.[71] Although the gradient retention times CHI(IAM) values and log k (IAM) values obtained for the acetophenone homologues did not show linear correlation with log P values due to the application of the acetonitrile gradient (see Figure 8a), the log K (IAM) values show a linear relationship with log P, as demonstrated in Figure 8b.

Therefore, the CHI(IAM) values were transformed to log K (IAM) values by eqs 11 and 12.

$$\text{Log } k\text{ (IAM)} = 0.046\text{ CHI(IAM)} + 0.42^{73} \quad (11)$$

$$\log K\text{ (IAM)} = 0.29e^{\log k\text{(IAM)}} + 0.70 \quad (12)$$

The constants were chosen to represent the CHI(IAM) values on the octanol/water log *P* scale.

We have observed a variation of retention behavior of the IAM column with charged compounds. We suggest conditioning the new columns by running several hundred fast gradients before use. After conditioning, the columns provided reproducible behavior for measuring up to 5000 compounds. The CHI(IAM) values for neutral compounds were very reproducible, practically within 2−4 CHI-(IAM) units throughout the column lifetime. To confirm the viability of the column, we suggest to check the CHI(IAM) values for three basic compounds (propranolol, 44−49; chlorpromazine, 58−62; and imipramin, 51−57) and three acidic compounds (warfarin, 28−22; diclofenac, 40−35; and ketoprofen, 22−18). We expect the values to be in these ranges. Figure 9 shows the change of the CHI(IAM) values for three neutral, three basic, and three acidic compounds that we run regularly to monitor the column aging.

Chromatographic Hydrophobicity Index (CHI) Measurements. In previous publications, we introduced a CHI that utilizes retention times from a rapid gradient reversed phase elution to measure lipophilicity.[73,74]

We used this method to determine CHI lipophilicity data at three pHs (pH2, pH 7.4, and pH 10.5) on Luna C18(2) column (Phenomenex, Cheshire, U.K.) 5 μm, with the dimensions of 50 × 3 mm.

At this point it should be noted that the CHI lipophilicity scale differs from the octanol/water lipophilicity scale, as revealed by the linear solvation equation.[76] It has been shown that the CHI lipophilicity is more similar to a water/alkane type of partition in that it is sensitive to the H-bond acidity of the compounds, whereas the octanol/water partition is not.

CHI values measured at three different pHs were also used to infer acid/base character of the compounds using the differences between the CHI values (delta CHI). Figure 10 illustrates the changes of CHI lipophilicity for acidic, basic, and neutral compounds.

As a measure of negative and positive charges present at physiological pH, we have generated a ΔCHInegchrg and a ΔCHIposchrg parameter from the difference of lipophilicity at pH 2 and pH 7.4 and pH 10.5 and pH 7.4, as described by the eqs 13 and 14:

$$\Delta\text{CHInegchrg} = \text{CHI}_2 - \text{CHI}_{7.4} \quad (13)$$

$$\Delta\text{CHIposchrg} = \text{CHI}_{10.5} - \text{CHI}_{7.4} \quad (14)$$

The ΔCHInegchrg and a ΔCHIposchrg values are positive numbers when negative or positive charges, respectively, are present. Large ΔCHI values indicate a higher proportion of the ionized form present at pH 7.4. When the difference in CHI values produces negative values, we substituted zero.

In Silico Calculation. The computed *C* log *P* data were calculated using software from ACD log *D* Suite, version 4.5 (ACDLabs, Toronto, Canada), and the pK_a values were calculated with pKalc 3.2 prediction module of Pallas system (CompuDrug Chemistry, Ltd., Hungary). The predominant charge state of compounds with measured CHI data was assigned with the help of these predicted pK_a values. Altogether, eight charge state groups were defined, as shown in Table 2. Classification was based on the pK_a values of acidic and basic groups. Zero means no acidic or basic groups are present. Increasing numbers (up to 7) denote decreasing acidic pK_a and increasing basic pK_a values. Thus, higher numbers signify higher % ionization of the compound at physiological pHs.

Model Building for VD. The statistical analyses were performed using JMP 3.2.5 version (SAS Institute, U.S.A.) statistical software.

For the visualization and interactive analysis of our results, Spotfire Decision Site program, Version 7.1.1 (Spotfire Inc., Somerville, U.S.A.) was used.

Stepwise regression analysis was used to determine the statistically significant parameters that can model VD.

To test the robustness of the models, the data sets were divided into a training set and a test set. The compounds were ranked based on their ascending VD values, and every fifth compound was allocated in the test set (30 compounds). The remaining ones were assigned into the training set (149 compounds). All the data were included in the models, and no outliers were removed from the data sets. MLR analysis was performed on the training set, and the model equations obtained were applied to calculate the VD values of the compounds in the test set.

The goodness of prediction has been presented by mean fold error and prediction accuracy (i.e., compounds predicted to have a VD value within a 2-fold error from the experimental value).

Fold error of prediction for VD test set values was calculated according to the following equation:

$$\text{fold error} = \text{antilog}\,(|\log \text{VD}_{\text{obs}} - \log \text{VD}_{\text{calc}}|) \quad (15)$$

Acknowledgment. Ferenc Hollósy is thankful to the Hungarian Scholarship Board for generously supporting his stay and research at GlaxoSmithKline Medicines Research Centre (Hungarian State Eötvös Scholarship 2-19-2-11-0656/2005). The authors are grateful to Dr. F. R. Obach (Pfizer) for the personal communication in which he identified the compounds in reference 72, so the published VD_{ss} data could be used in our models.

Supporting Information Available: Literature VD and PPB data of the investigated compounds, including their CAS numbers and references. This material is available free of charge via the Internet at http://pubs.acs.org.

References

(1) Smith, D. A.; Jones, B. C.; Walker, D. K. Design of drugs involving the concepts and theories of drug metabolism and pharmacokines. *Med. Res. Rev.* **1996**, *16*, 243−266.
(2) Avdeef, A. Absorption and drug development; Wiley: Hoboken, NJ, 2003.
(3) Van de Waterbeemd, H.; Smith, D. A. Relations of molecular properties with drug disposition: The cases of gastrointestinal absorption and brain penetration. In *Pharmacokinetic Optimization in Drug Research*; Testa, B., van de Waterbeemd, H., Folkers, G., Guy, R., Eds.; Wiley-VCH: Weinheim, Germany, 2001; pp 52−64.
(4) Van de Waterbeemd, H.; Lennernäs, H.; Artursson, P. *Drug bioavailability*; Wiley-VCH: Weinheim, Germany, 2003.
(5) Kerns, E. H. High throughput physicochemical profiling for drug discovery. *J. Pharm. Sci.* **2001**, *90*, 1838−1858.
(6) Kerns, E. H.; Di, L. Physicochemical profiling: overview of the screens. *DDT Technologies* **2004**, *4*, 343−348.
(7) Sawada, Y.; Hanano, M.; Sugiyama, Y.; Harashima, H.; Iga, T. Prediction of the volume of distribution of basic drugs in human based on data from animals. *J. Pharmacokinet. Biopharm.* **1984**, *12*, 587−596.
(8) Wajima, T.; Fukumura, K.; Yano, Y.; Oguma, T. Prediction of human pharmacokinetics from animal data and molecular parameters using multivariate regression analysis: volume of distribution at steady state. *J. Pharm. Pharmacol.* **2003**, *55*, 939−949.
(9) Wilkinson, G. R. Pharmacokinetics: the dynamics of drug absorption, distribution, and elimination. *Goodman & Gillman's the pharmacological bases of therapeutics*, 10th ed.; Hardman, J. G., Limbird, L. E., Gillman, A. G., Eds.; McGraw-Hill: New York, 2001; pp 20−22.
(10) Kwon, Y. *Handbook of essential pharmacokinetics, pharmacodynamics and drug metabolism for industrial scientists*; Kluwer Academic/Plenum Publisher: New York, 2001; p 106.
(11) Øie, S.; Tozer, T. N. Effect of altered plasma protein binding on apparent volume of distribution. *J. Pharm. Sci* **1979**, *68*, 1203−1205.
(12) Boxenbaum, H. Ronfeld, R. Interspecies pharmacokinetic scaling and the Dedrick plots. *Am. J. Physiol.* **1983**, *245*, 768−775.
(13) Boxenbaum, H. Interspecies pharmacokinetic scaling and the evolutionary-comparative paradigm. *Drug Metab. Rev.* **1984**, *15*, 1071−1121.

(14) Hutchaleeha, A.; Chow, H. H.; Mayersohn, M. Comparative pharmacokinetics and interspecies scaling of amphotericin B in several mammalian species. *J. Pharm. Pharmacol.* **1997**, *49*, 178−183.
(15) Lave, T.; Coassolo, P.; Reigner, B. Prediction of hepatic metabolic clearance based on interspecies allometric scaling techniques and in vitro-in vivo correlations. *Clin. Pharmacokinet.* **1999**, *36*, 211−231.
(16) Poulin, P.; Theil, F. P. Prediction of pharmacokinetics prior to in vivo studies. I. Mechanism-based prediction of volume of distribution. *J. Pharm. Sci.* **2000**, *91*, 129−156.
(17) Poulin, P.; Theil, F. P. Prediction of pharmacokinetics prior to in vivo studies. II. Generic physiologically based pharmacokinetic models of drug disposition. *J. Pharm. Sci.* **2002**, *91*, 1358−1370.
(18) Ritschel, W. A.; Vachharajani, N. N.; Johnson, R. D.; Hussain, A. S.; The allometric approach for interspecies scaling of pharmacokinetic parameters. *Comp. Biochem. Physiol., C: Pharmacol., Toxicol. Endocrinol.* **1992**, *103*, 249−253.
(19) Mahmood, I.; Balian, J. D. Interspecies scaling: predicting pharmacokinetic parameters of antiepileptic drugs in humans from animals with special emphasis on CL. *J. Pharm. Sci.* **1996**, *85*, 411−414.
(20) Obach, R. S.; Baxter, J. G.; Liston, T. E.; Silber, B. M.; Jones, B. C; MacIntyre, F. Rance, D. J.; Wastall, P. The prediction of human pharmacokinetic parameters from preclinical and in vitro metabolism data. *J. Pharmacol. Exp. Ther.* **1997**, *283*, 46−58.
(21) Karalis, V.; Claret, L.; Iliadis, A.; Macheras, P. Fractal volume of distribution: it scales proportionally to the body mass. *Pharm. Res.* **2001**, *18*, 1056−1060.
(22) Karalis, V.; Macheras, P. Drug disposition viewed in terms of the fractal volume of distribution. *Pharm. Res.* **2002**, *19*, 697−704.
(23) Krishnan, K.; Andersen, M. E. Physiologically based pharmacokinetic modelling in toxicology. In *Principle and Methods of Toxicology*; Hayes, W., Ed.; Taylor & Francis: Philadelphia, PA, 2001; pp 193−241.
(24) Poulin, P.; Beliveau, M.; Krishnan, K. Mechanistic animal-replacement approaches for predicting pharmacokinetics of organic chemicals. In *Toxicity Assessments Alternatives: Methods, Issues, Opprotunities*; Salem, H., Katz, S.A., Eds.; Humana Press: Totowa, NJ, 1999; pp 115−139.
(25) Theil, F. P.; Guentert, T. W.; Haddad, S.; Poulin, P. Utility of physiologically based pharmacokinetic models to drug development and rational drug discovery candidate selection. *Toxicol. Lett.* **2003**, *138*, 29−49.
(26) Yokogawa, K.; Ishizaki, J.; Ohkuma, S.; Miyamoto, K. Influence of the lipophilicity and lysosomal accumulation on tissue distribution kinetics of basic drugs: A physiologically based pharmacokinetic model. Methods find. *Exp. Clin. Pharmacol.* **2002**, *24*, 81−93.
(27) Van de Waterbeemd, H. High-throughput and in silico techniques in drug metabolism and pharmacokinetics. *Curr. Opin. Drug Discovery Dev.* **2002**, *5*, 33−43.
(28) Van de Waterbeemd, H.; Gifford, E. ADMET in silico modelling: towards prediction paradise? *Nat. Rev. Drug Discovery* **2003**, *2*, 192−204.
(29) Dickins, M.; Van de Waterbeemd, H. Simulation models for drug disposition and drug interactions. *BIOSILICO* **2004**, *2*, 3845.
(30) Poulin, P.; Theil, F. P. A priori prediction of tissue: plasma partition coefficients of drugs to facilitate the use of physiologically-based pharmacokinetic models in drug Discovery. *J. Pharm. Sci.* **2000**, *89*, 16−35.
(31) Gleeson, P.; Waters, N. J.; Paine, S. W.; Davis, A. M. In silico human and rat V_{ss} quantitative structure−activity relationship models. *J. Med. Chem.* **2006**, *49*, *1953*−1963.
(32) Lombardo, F.; Obach, R. S.; DiCapua, F. M.; Bakken, G. A.; Lu, J.; Potter, D. M.; Gao, F.; Miller, M. D.; Zhang, Y. Hybrid mixture discriminant analysis-random forest computational model for the prediction of volume of distribution of drugs in human. *J. Med. Chem.* **2006**, *49*, *2262*−2267.
(33) Balaz, S.; Lukacova, V. A model-based dependence of human tissue/blood partition coefficients of chemicals on lipophilicity and tissue composition. *Quant. Struct.-Act. Relat.* **1999**, *18*, 361−368.
(34) Haddad, S.; Poulin, P.; Krishnan, K. Relative lipid content as the sole mechanistic determinant of the adipose tissue:blood partition coefficients of highly lipophilic organic chemicals. *Chemosphere* **2000**, *40*, 839−843.
(35) Beliveau, M.; Krishnan, K. Concentration dependency of rat blood: air partition coefficients of some volatile organic chemicals. *J. Toxicol. Environ. Health* **2000**, *60*, 377−389.
(36) Meulenberg, C. J. W.; Vijverberg, H. P. M. Empirical relations predicting human rat tissue:air partition coefficients of volatile organic chemical compounds. *Toxicol. Appl. Pharmacol.* **2000**, *165*, 206−216.
(37) Payne, P. P.; Kenny, L. C.; Comparison of models for estimation of biological partition coefficients. *J. Toxicol. Environ. Health* **2002**, *65*, 897−931.
(38) Theil, F. P.; Guentert, T. W.; Haddad, S.; Poulin, P. Utility of physiologically based pharmacokinetic models to drug development and rational drug discovery candidate selection. *Toxicol. Lett.* **2003**, *138*, 29−49.
(39) Kratochwill, N.; Huber, W.; Muller, F.; Kansy, M.; Gerber, P. R. Predicting plasma protein binding of drugs—revisited. *Curr. Opin. Drug Discovery Dev.* **2004**, *4*, 507 -512
(40) Testa, B.; Crivori, P.; Reist, M.; Carrupt, P. A. The influence of lipophilicity on the pharmacokinetic behavior of drugs: Concepts and examples. *Perspect. Drug Discovery Des.* **2000**, *19*, 179−211.
(41) Poulin, P.; Schoenlein, K.; Theil, F. P. Prediction of adipose tissue: plasma partition coefficients for structurally unrelated drugs. *J. Pharm. Sci.* **2001**, *90*, 436−447.
(42) Smith, D. A.; Van de Waterbeemd, H.; Walker, D. K. *Pharmacokinetics and metabolism in drug design*; Wiley-VCH: Weinheim, Germany, 2001; pp 123132.
(43) Lombardo, F.; Obach, R. S.; Shalaeva, M. Y.; Gao, F. Prediction of volume of distribution values in humans for neutral and basic drugs using physicochemical measurements and plasma protein binding data. *J. Med. Chem.* **2002**, *45*, 2867−2876.
(44) Lombardo, F.; Obach, R. S.; Shalaeva, M. Y.; Gao, F. Prediction of humane volume of distribution values for neutral and basic drugs. 2. Extended data set and leave-class-out statistics. *J. Med. Chem.* **2004**, *47*, 1242−1250.
(45) Rowland, M.; Tozer, T. N. *Clinical Pharmacokinetics. Concepts and Applications*; Lippincott, Williams and Wilkins: Philadelphia, PA, 1995; pp 143−155.
(46) Lombardo, F.; Shalaeva, M. Y.; Tupper, K. A.; Gao, F. *E* log D_{oct}: A tool for lipophilicity determination in drug discovery. 2. basic and neutral compounds. *J. Med. Chem.* **2001**, *44*, 2490−2497.
(47) Loidl-Stahlhofen, A. A.; Eckert, T.; Hartmann, M. Schottner: Solid-supported lipid membranes as a tool for determination of membrane affinity: high-throughput screening of a physicochemical parameter. *J. Pharm. Sci.* **2001**, *90*, 599−606.
(48) Willmann, S.; Lippert, J.; Severstre, M.; J. Solodenk; Schmitt, W. PK-Sim: a physiologically based pharmacokinetic "whole-body" model. *BIOSILICO* **2003**, *1*, 121−124.
(49) *PK-SIMsoftware*. http://www.bayertechnology.com/produkte/43_PK-Sim_Software_Product_PBPK_Physiologically_Based_Pharmacokinetic_Simulations.php (last accessed Oct 2006).
(50) Brodie, B. B.; Kurtz, H.; Schanker, L. J. The importance of dissociation constants and lipid solubility on influencing the passage of drugs into the CSF. *J. Pharmacol. Exp. Ther.* **1960**, *130*, 20−25.
(51) Physical Chemistry Composition of Blood Hematology Somatometric Data. *Geigy Scientific Tables*; Lentner, C., Ed.; CIBA-GEIGY, Ltd.: Basel, 1984; Vol 3, p 135.
(52) Herve, F.; Urien, S.; Albengres, E.; Duche, J. C. Drug binding in plasma. A summary of recent trends in the study of drug and hormone binding. *Clin. Phamacokinet.* **1994**, *26*, 44−58.
(53) Clarke's isolation and identification of drugs, 2nd ed.; Pharmaceutical Press: London, 1986.
(54) Vozeh, S.; Schmidlin, O.; Taeschner, W. Pharmacokinetic drug data. *Clin. Pharmacokinet.* **1988**, *15*, 254−282.
(55) Goodman, L. S.; Gilman, A. G. *The pharmacological basis of therapeutics*, 9th ed.; McGraw-Hill: New York, 1996.
(56) GSK in-house data. These data were derived partly from experiments carried out in former SmithKlineBeecham as well as in former Glaxo Wellcome and partly from the present GSK database records in the time period of 1996−2001. (VD reference file).
(57) Dollery, C. *Therapeutic drugs*, 2nd ed.; Churchill Livingstone: Edinburgh, New York, 1999.
(58) Jhee, S. S.; Shiovitz, T.; Crawford, A. W.; Cutler, N. R. Pharmacokinetics and pharmacodynamics of the triptan antimigraine agents. A comparative review. *Clin. Pharmacokinet.* **2001**, *40*, 189−205.
(59) Gilman, A. G.; Goodman, L. S.; Hardman, J. G.; Limbird, L. E. *The pharmacological basis of therapeutics*, 8th ed.; MacGraw-Hill: New York, 1990.
(60) Boxenbaum, H. Comparative pharmacokinetics of benzodiazepines in dog and man. *J. Pharm. Biopharm.* **1982**, *10*, 411−426.
(61) Kratochwil, N. A.; Huber, W.; Muller, F.; Kansy, M.; Gerber, P. R. Predicting plasma protein binding of drugs: a new approach. *Biochem. Pharmacol.* **2002**, *64*, 1355−1374.
(62) Yamazaki, K.; Kanaoka, M. Computational prediction of the plasma protein-binding percent of diverse pharmaceutical compounds. *J. Pharm. Sci.* **2004**, *93*, 1480−1494.
(63) Karalis, V.; Tsantili-Kakoulidou, A.; Macheras, P. Quantitative structure−pharmacokinetic relationships for disposition parameters of cephalosporins *Eur. J. Pharm. Sci.* **2003**, *20*, 115−123.
(64) Derendorf, H. Pharmacokinetic and pharmacodynamic properties of inhaled corticosteroids in relation to efficacy and safety. *Resp. Med.* **1997**, *91*, 22−28.

(65) Saiakhov, R. D.; Stefan, L. R.; Klopman, G. Multiple computer-automated structure evaluation model of the plasma protein binding affinity of diverse drugs. *Perspect. Drug Discovery Des*. **2000**, *19*, 133−155.
(66) Lombardo, F.; Obach, R. S.; DiCapua, F. M.; Bakken, G. A.; Lu, J.; Potter, D. M.; Gao, F.; Miller, M. D.; Zhang, Y. Hybrid mixture discriminant analysis-random forest computational model for the prediction of volume of distribution of drugs in human. *J. Med. Chem.* **2006**, *49* (7), 2262−2267.
(67) Brogden, R. N.; Campoli-Richards, D. M. Cefixime A review of its antibacterial activity, pharmacokinetic properties and therapeutic potential. *Drugs* **1989**, *38* (4), 524−550.
(68) Young, M. A.; Aarons, L.; Toon, S. Pharmacokinetics of the enantiomers of flurbiprofen in patients with rheumatoid arthritis. *Br. J. Clin. Pharm.* **1991**, *31*, 102−104.
(69) Davies, N. M.; Anderson, K. E. Clinical pharmacokinetics of naproxen. *Drug Dispos. Dev.* **1997**, *32* (4), 268−293.
(70) Caruso, I.; Corvi, G.; Fuccella, L. M.; Moro, E.; Saccetti, G.; Tamassia, V.; Tosolini, G. P. Pharmacokinetic studies of indoprofen in healthy volunteers and in patients. *Int. J. Clin. Pharmacol.* **1977**, *15* (9), 411−416.
(71) Valko, K.; Du, C. M.; Bevan, C. D.; Reynolds, D .P.; Abraham, M. H. Rapid gradient HPLC method for measuring drug interactions with immobilized artificial membrane: comparison with other lipophilicity measures. *J. Pharm. Sci.* **2000**, *89*, 1085−1096.
(72) Valko, K.; Nunhuck, S.; Bevan, C.; Abraham, M. H.; Reynolds, D. P. Fast gradient HPLC method to determine compounds binding to human serum albumin. Relationships with octanol/water and immobilized artificial membrane lipophilicity. *J. Pharm. Sci.* **2003**, *92*, 2236−2248.
(73) Valko, K. Measurements of lipophilicity and acid/base character using HPLC methods. In *Biotechnology: Pharmaceutical Aspects*. *Pharmaceutical Profiling in Drug Discovery for Lead Selection*; Borchardt, R. T., Kerns, E. H., Lipinski, C. A., Thakker, D. R., Wang, B., Eds.; AAPS press: Washington DC, 2004; Vol 1, pp 127−182.
(74) Herbette, L. G.; Chester, D. W.; Rhodes, D. G. Structural analysis of drug molecules in biological membranes. *Biophys. J.* **1986**, *49*, 91−94.
(75) Kaliszan, R.; Nasal, A.; Bucinski, A. Chromatographic hydrophobicity parameter determined on an immobilized artificial membrane column: relationships to standard measures of hydrophobicity and bioactivity. *Eur. J. Med. Chem.* **1994**, *29*, 163−170.
(76) Valko, K.; Bevan, C.; Reynolds, D. Chromatographic hydrophobicity index by fast gradient RP-HPLC: A high-throughput alternative to log *P*/log *D*. *Anal. Chem.* **1997**, *69*, 2022−2029.

JM050957I